

Enomoto, "Antihydrogen production in cusp trap" review

Seoul National University

15.Oct.2018

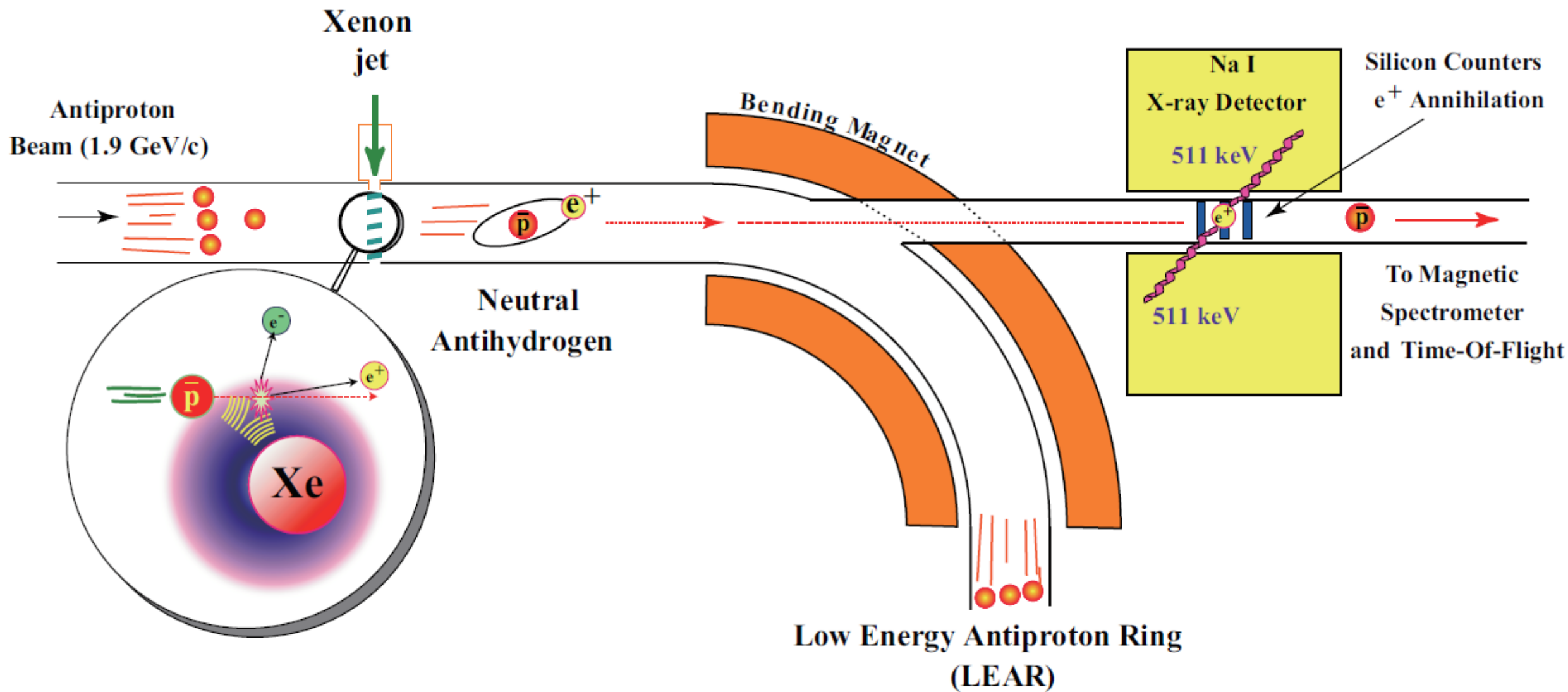


Figure 1.1: A schematic drawing of the experimental setup in which the first antihydrogen atoms were observed by PS210 collaboration.

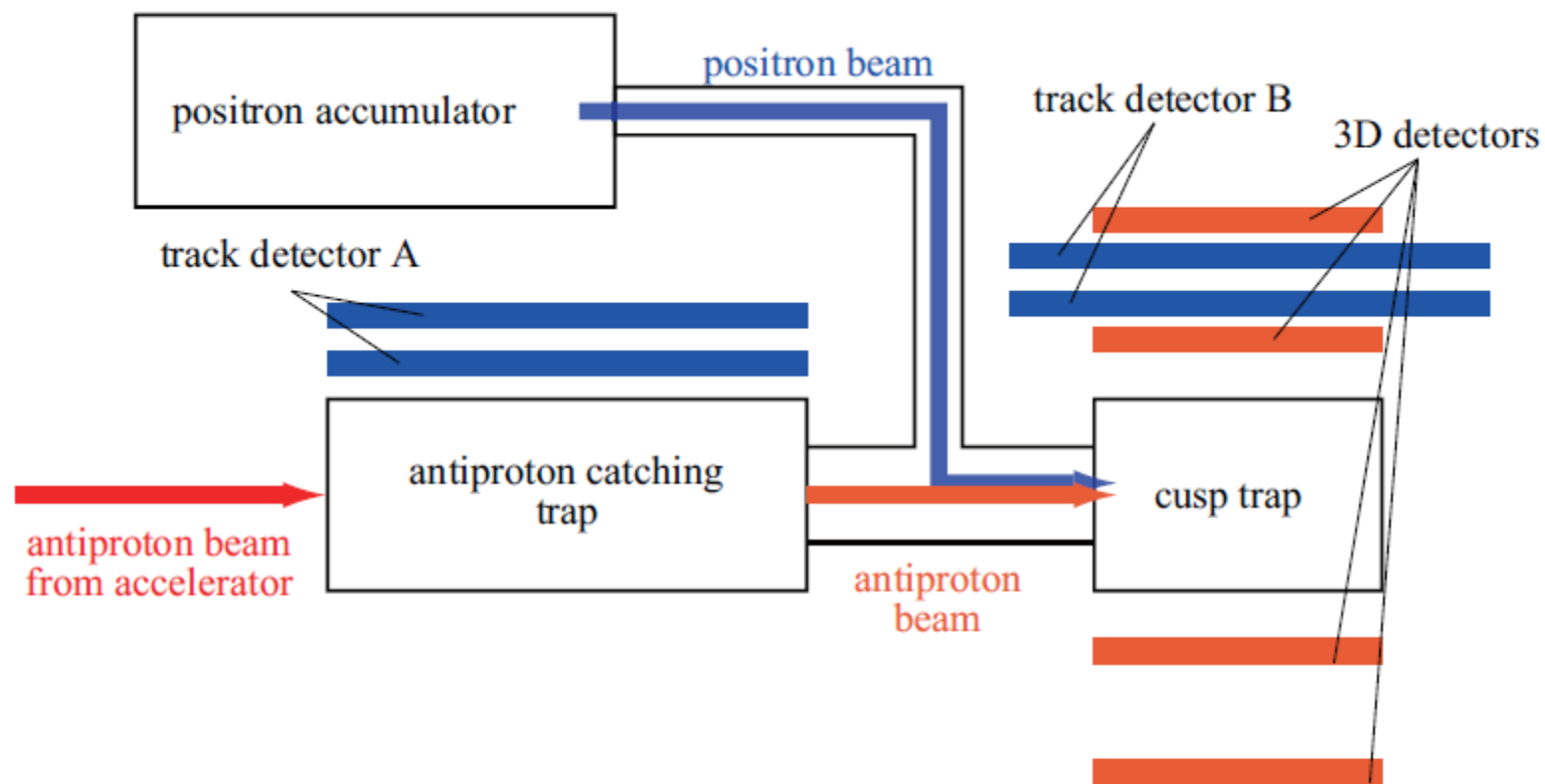
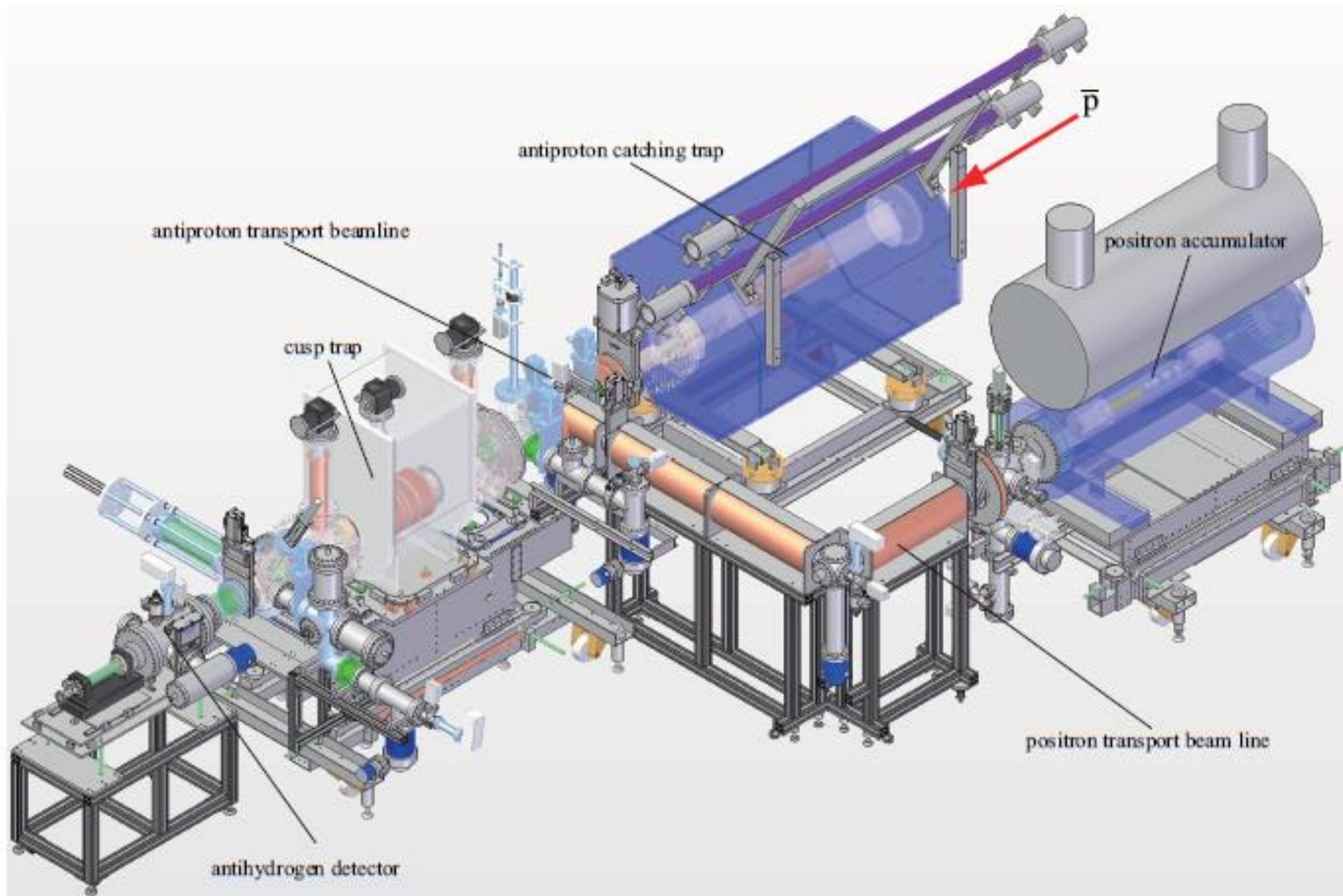
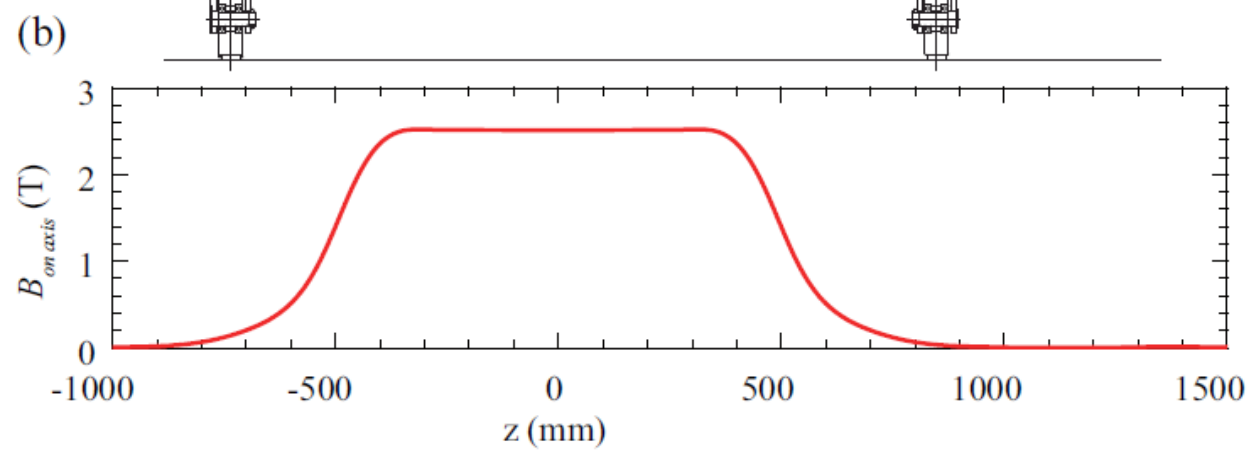
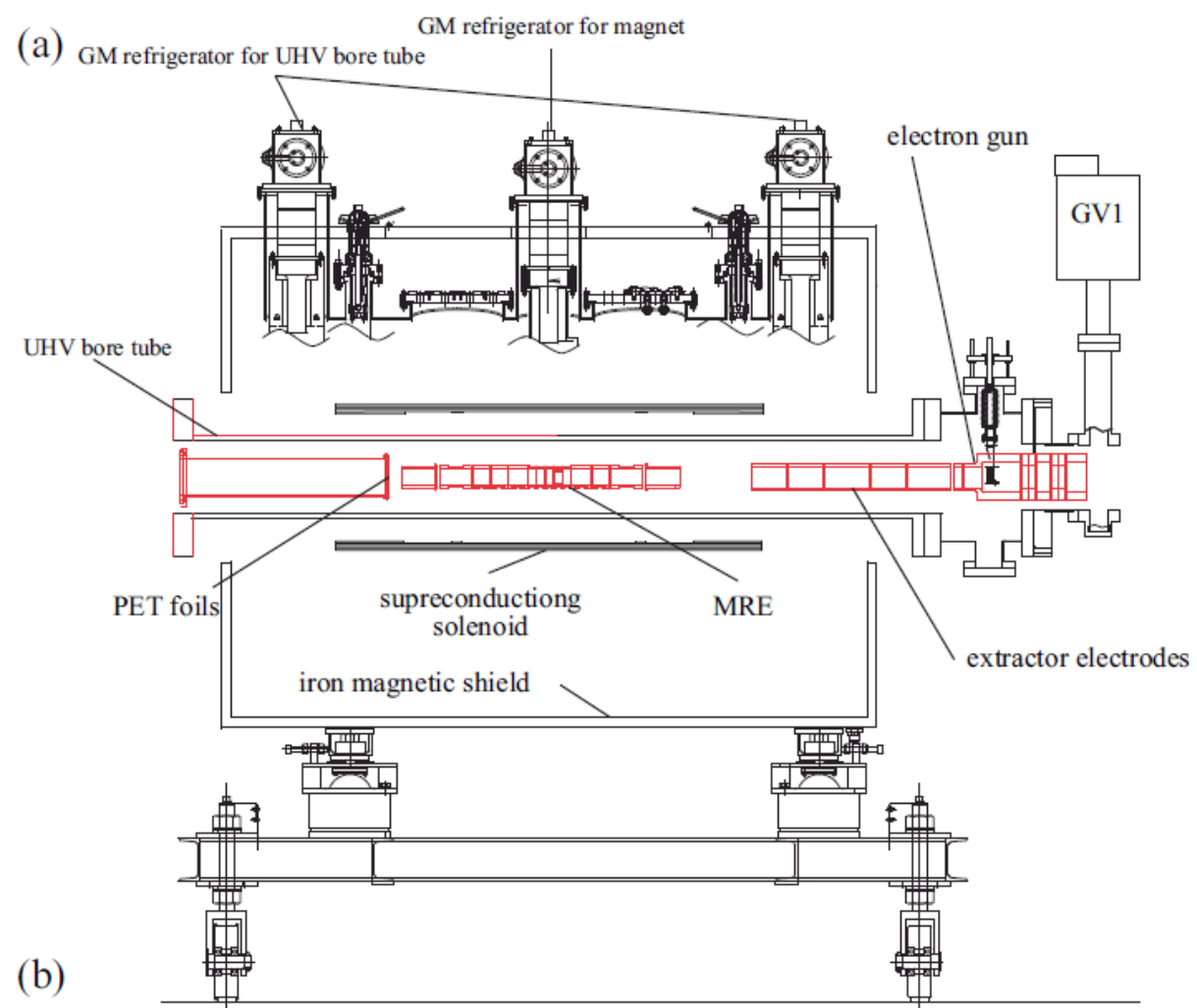


Figure 3.1: A schematic drawing of the apparatus. It consists of an antiproton catching trap, a positron accumulator, transport beamlines, a cusp trap and detectors.





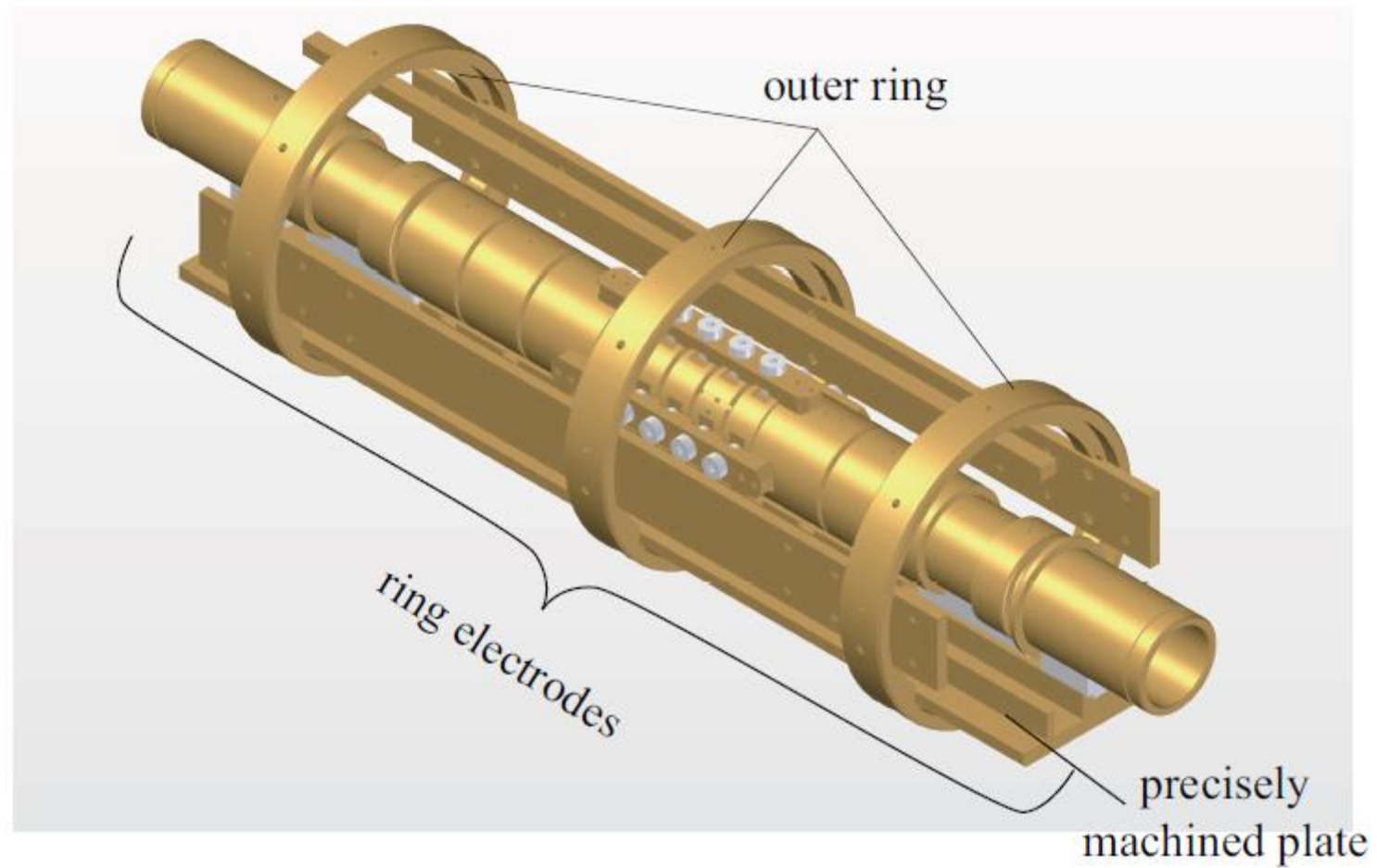


Figure 3.7: An isometric view of the MRE of the antiproton catching trap. The 14 ring electrodes, which are made of gold-plated oxygen free copper, are aligned on the precisely machined plate and the plate is connected to three outer rings which contact to the bore tube and hold the whole set.

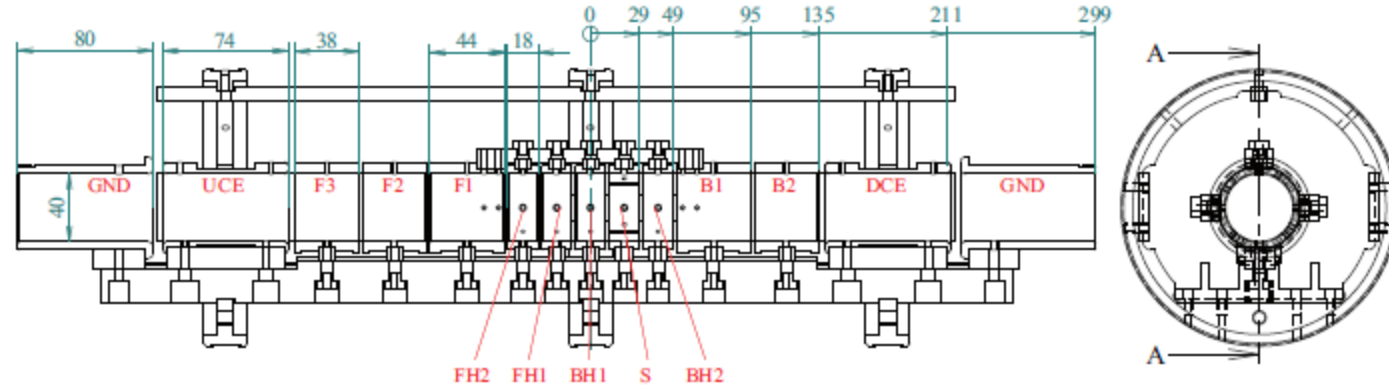


Figure 3.8: A cross sectional drawing of the MRE of the antiproton catching trap. The DCE and the UCE are used to capture energetic antiprotons by applying high voltage. The five electrodes, FH2, FH1, BH1, S, and BH2 are used to make a harmonic potential. The S electrode (azimuthally four-segmented electrode) are used to compress antiproton cloud by applying a rotating electric field.

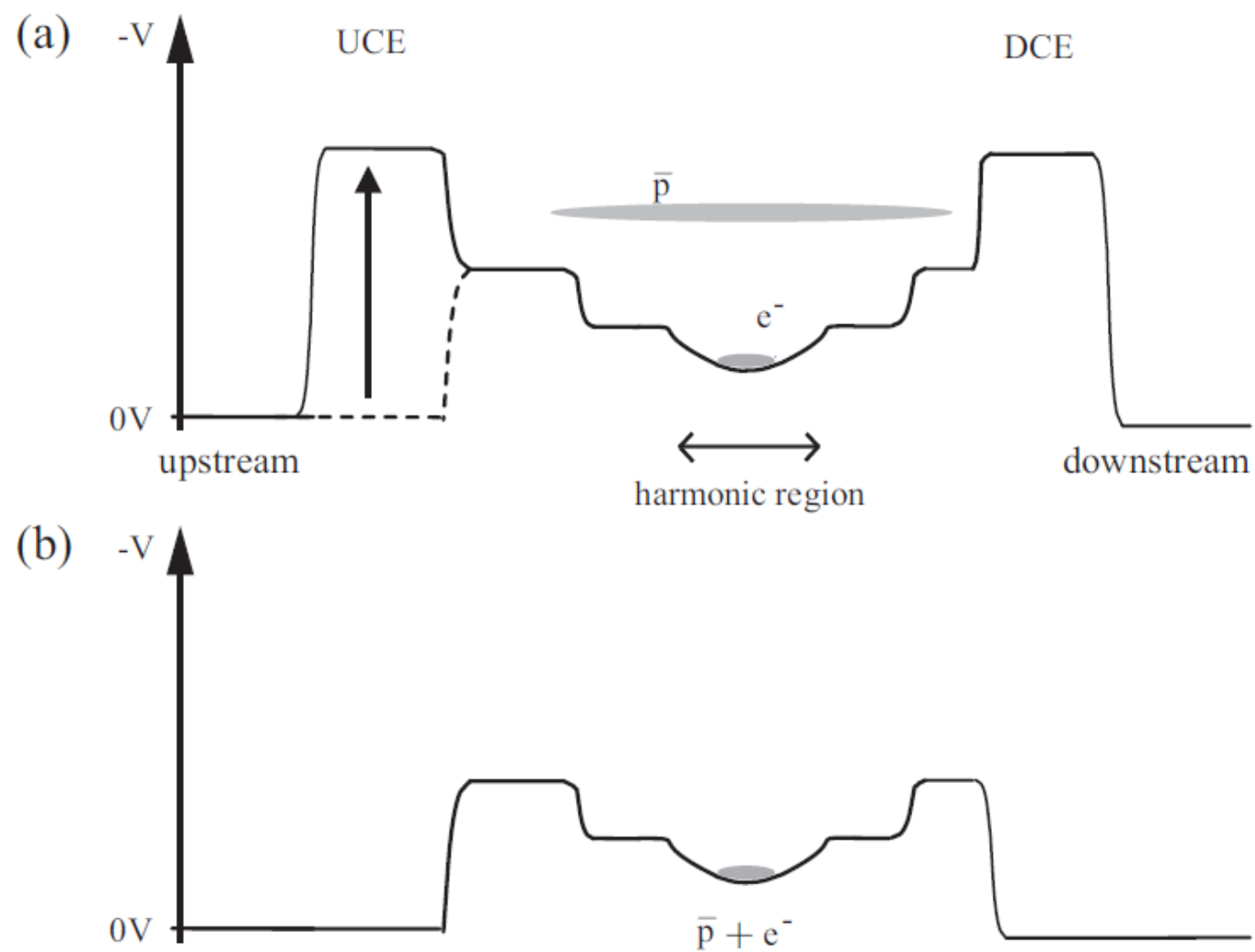


Figure 3.9: A schematic drawing of potential configurations for capture and cool the energetic antiprotons. The injected antiprotons are reflected back by the potential wall made by the DCE. Then the UCE is biased before the antiprotons reach the UCE and they are cooled by the pre-loaded electrons (a). After about 40 s from the injection of the energetic antiprotons, high voltages applied on the UCE and the DCE are changed to 0 V (b).

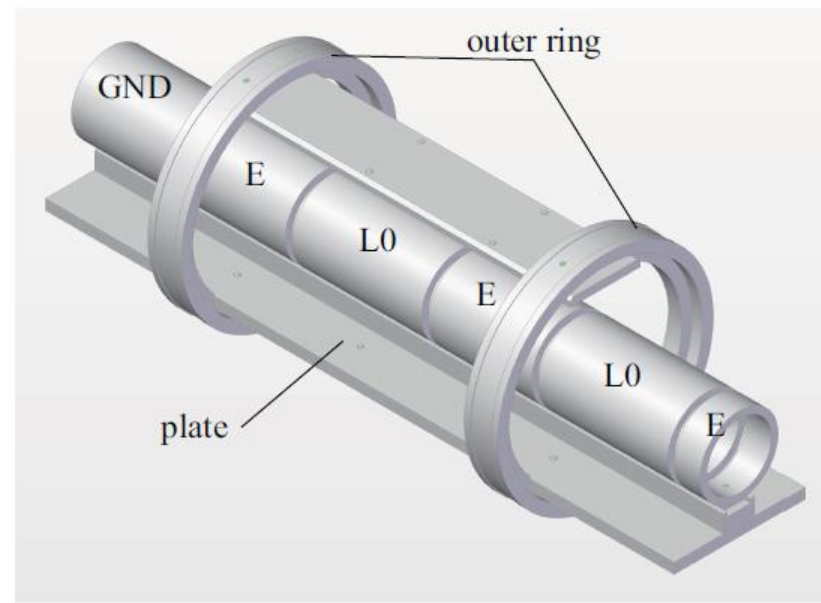


Figure 3.10: An isometric view of the extractor electrodes of the antiproton catching trap, which consist of six ring electrodes of aluminium alloy. Each electrode is aligned on a plate and the plate is connected to two outer rings which contact to the bore tube and hold the whole set.

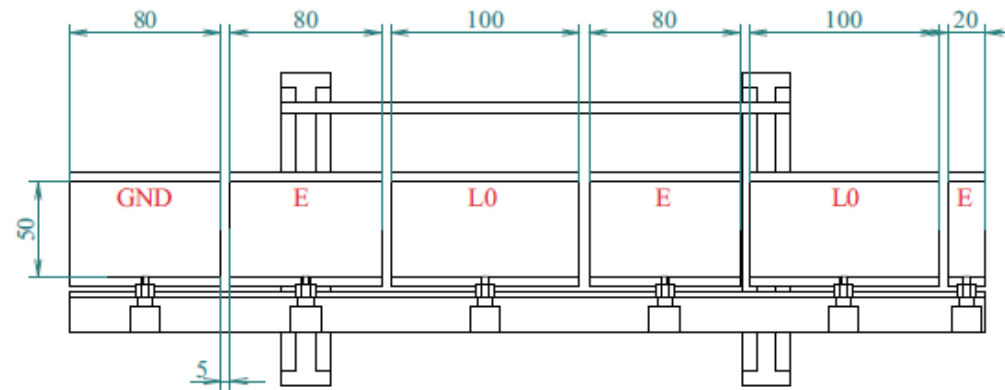
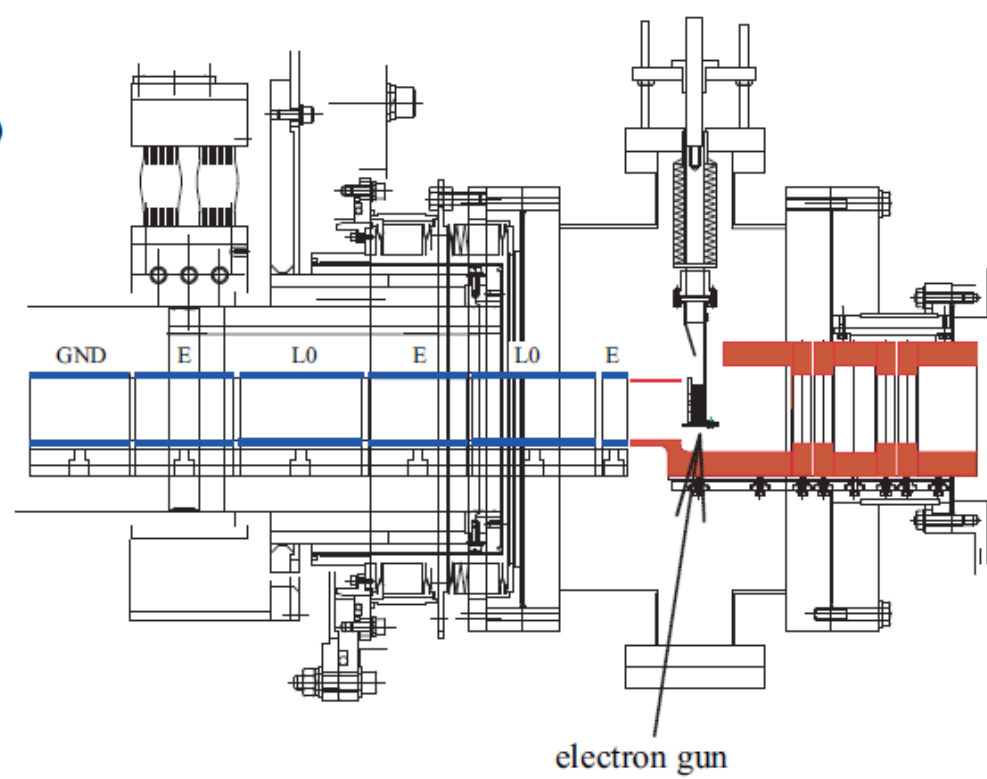
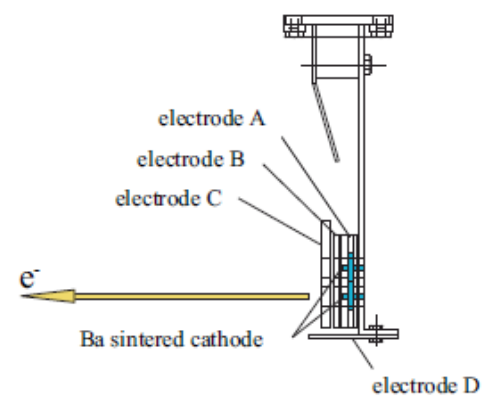


Figure 3.11: A cross sectional drawing of the extractor electrodes of the antiproton catching trap. The inner diameter of the six electrodes are 50 mm.

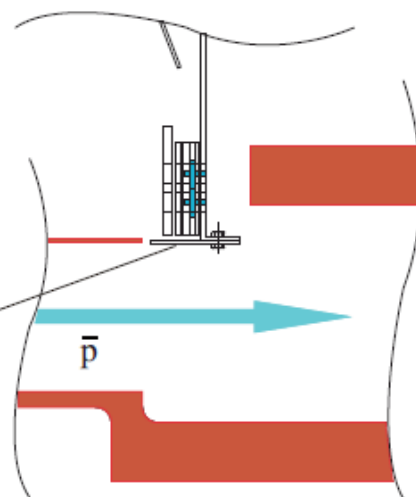
(a)



(b)



(c)



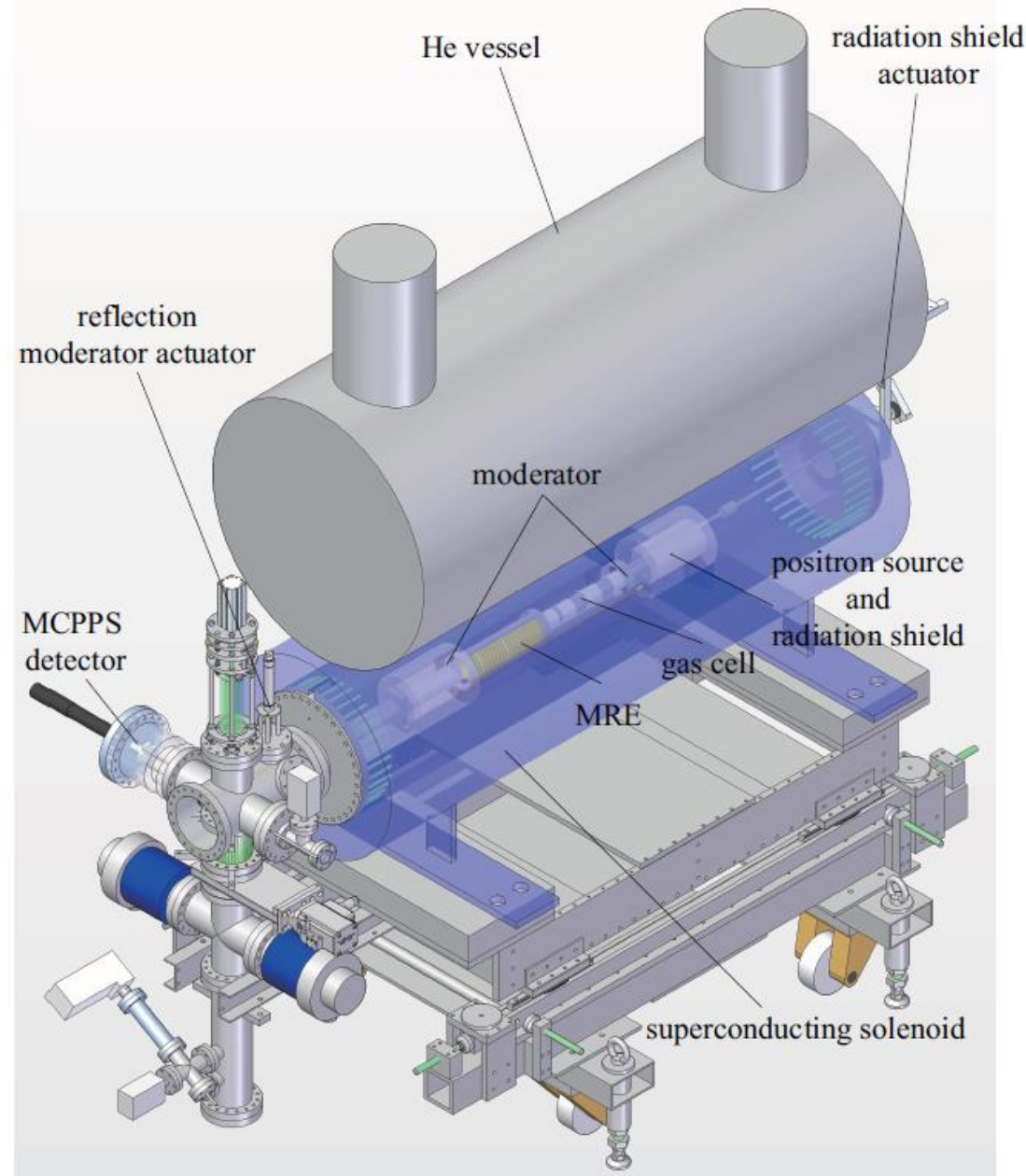


Figure 3.17: An isometric view of the positron accumulator. The source, the MRE, the gas cell and the moderators are housed in the superconducting solenoid. An MCPPS detector is attached downstream side of the solenoid to monitor extracted positrons.

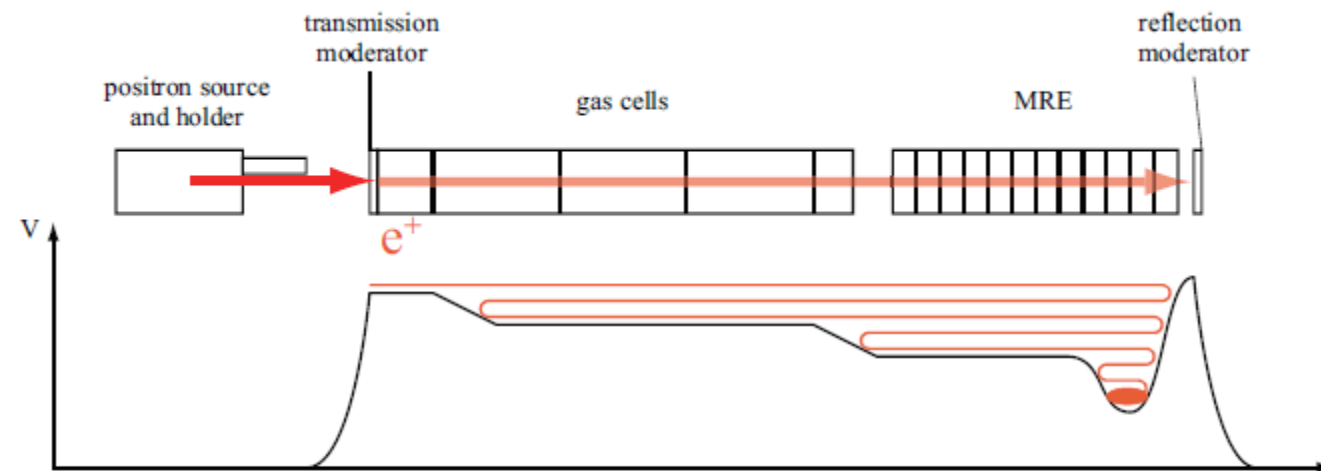


Figure 3.16: A schematic drawing of the positron accumulator and an electric potential. Positrons from the source are thermalized by the moderators and accumulated in the potential well made by the MRE via collisions with nitrogen buffer gas.

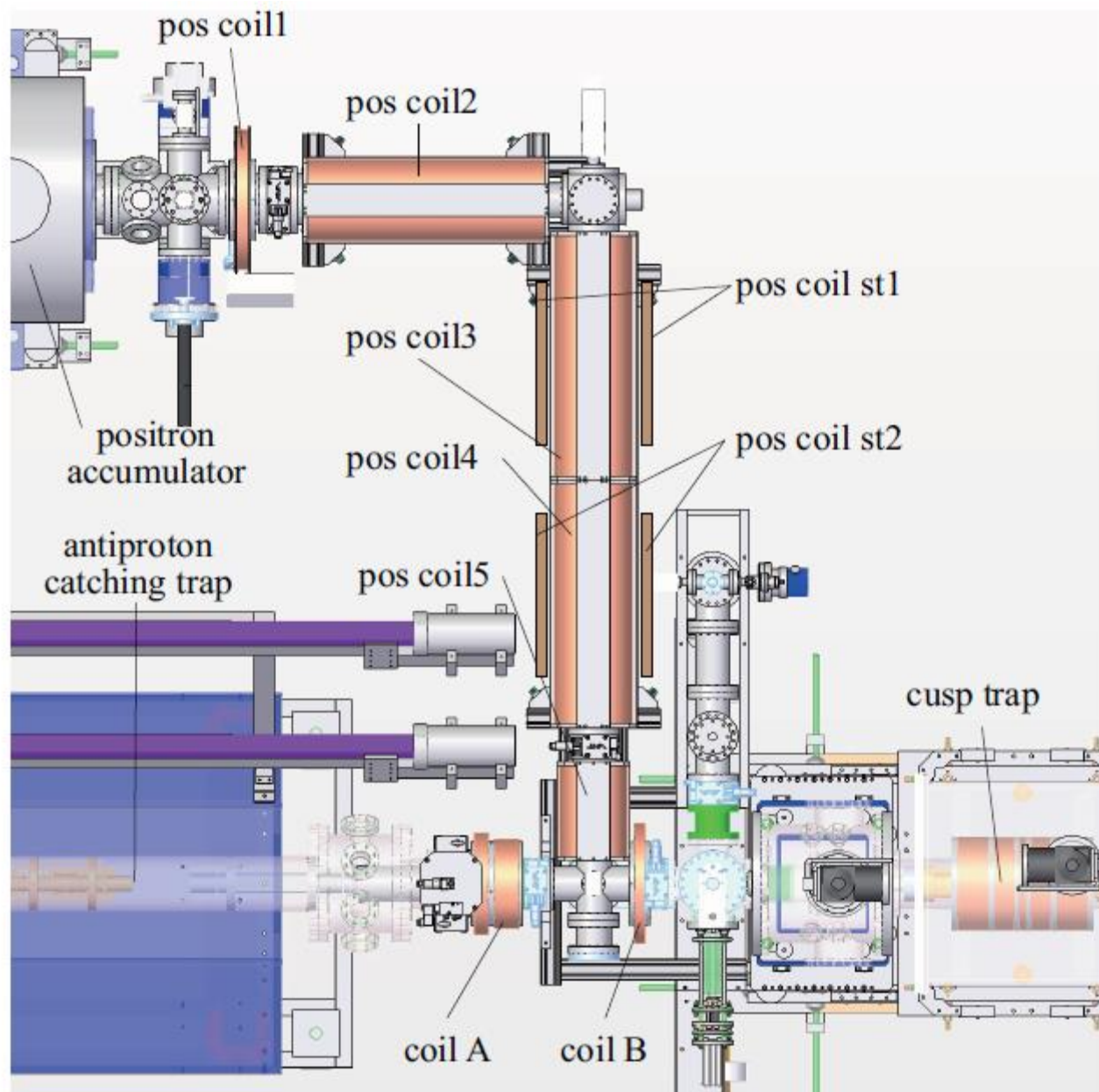


Figure 3.29: Configuration of the coils for the transport of the ultra-low energy antiproton and positron beams.

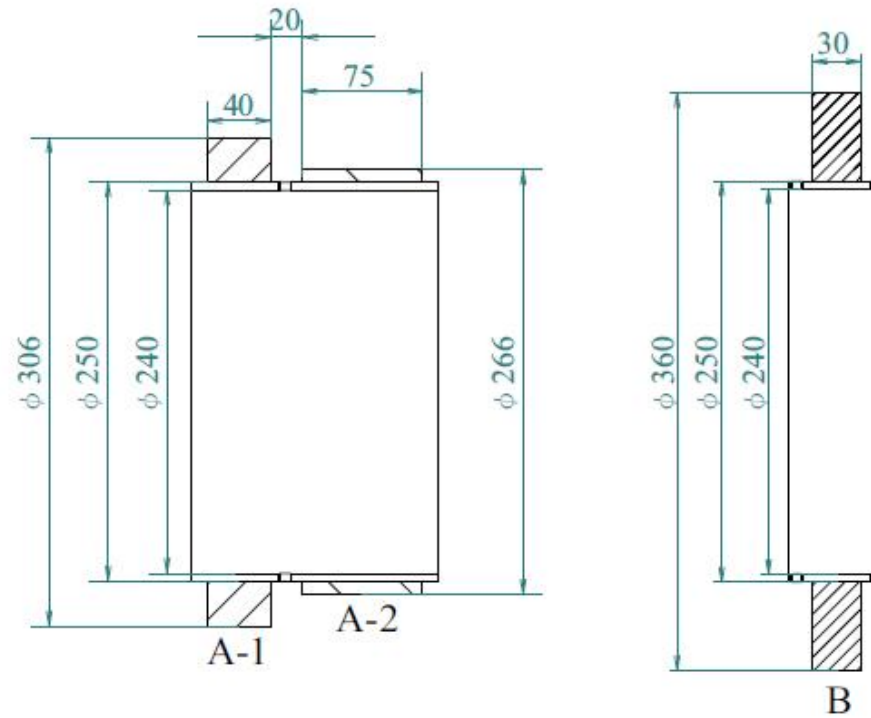
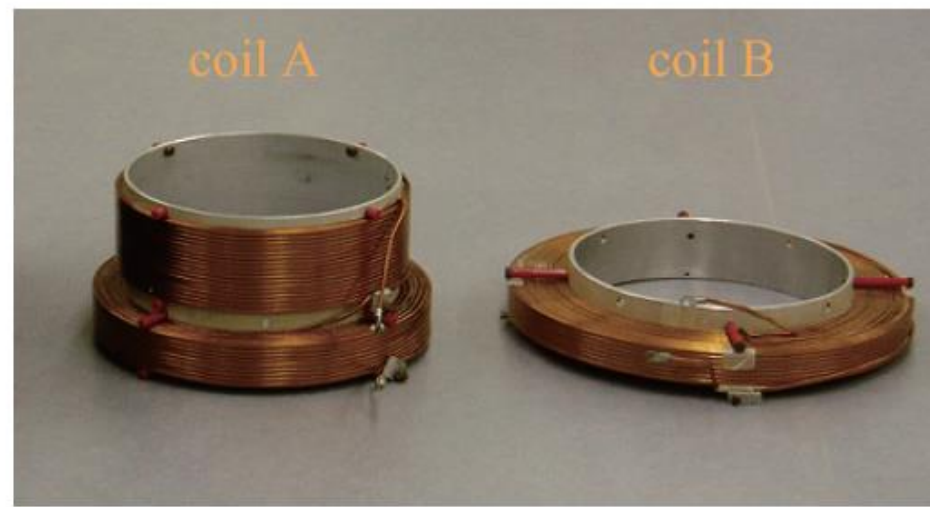
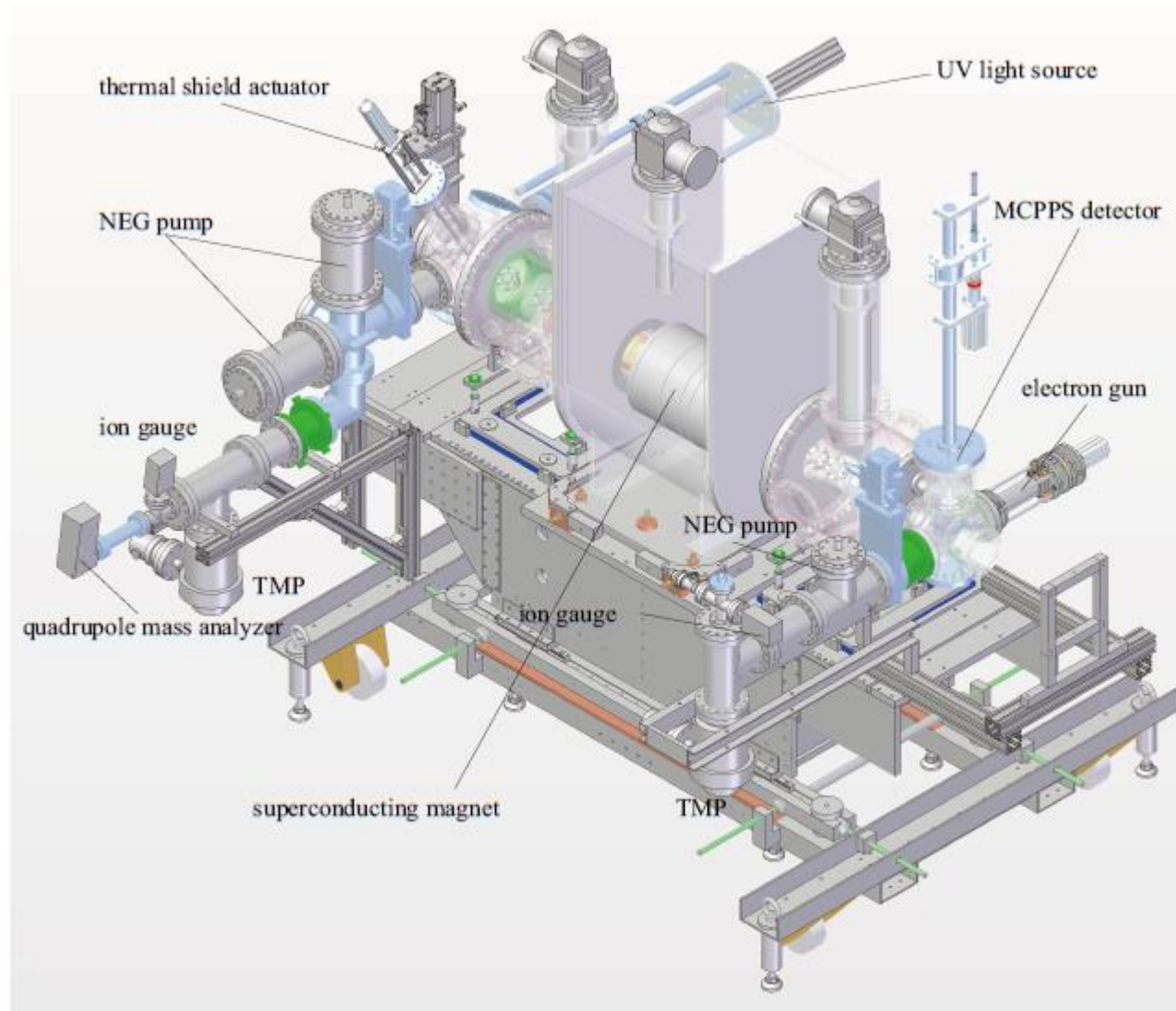


Figure 3.30: A photograph (top) and a cross sectional drawing (bottom) of the coils for the antiproton beam transport.

Cusp Trap



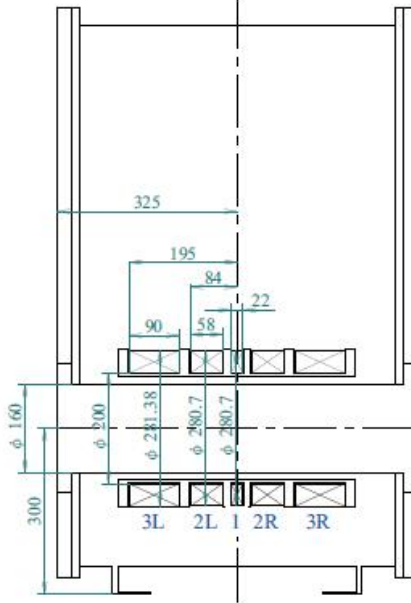


Figure 3.39: A cross sectional drawing of the superconducting magnet of the cusp trap. The magnet consists of five coils whose inner diameter is 200 mm.



Figure 3.40: A photograph of the superconducting magnet of the cusp trap.

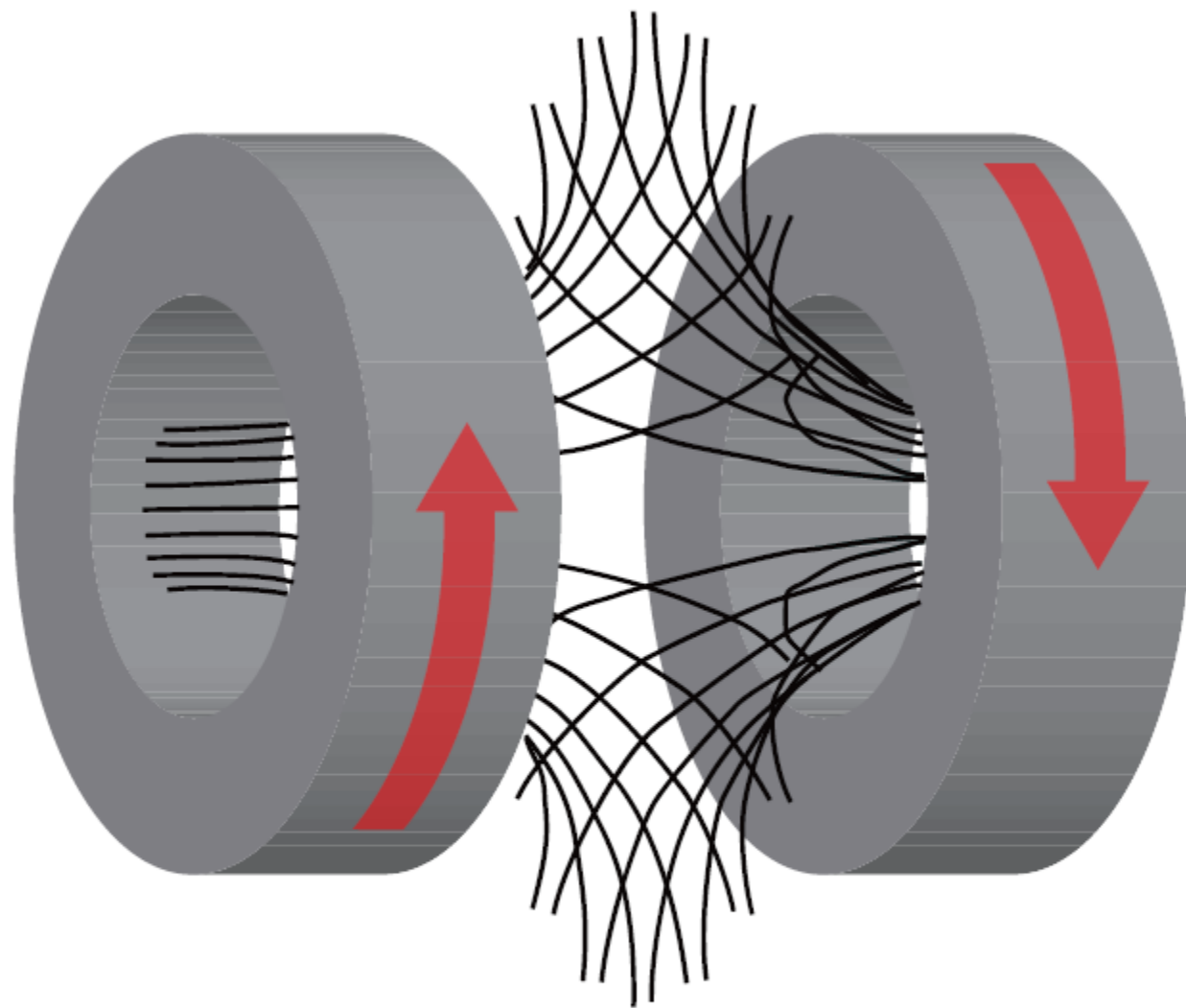
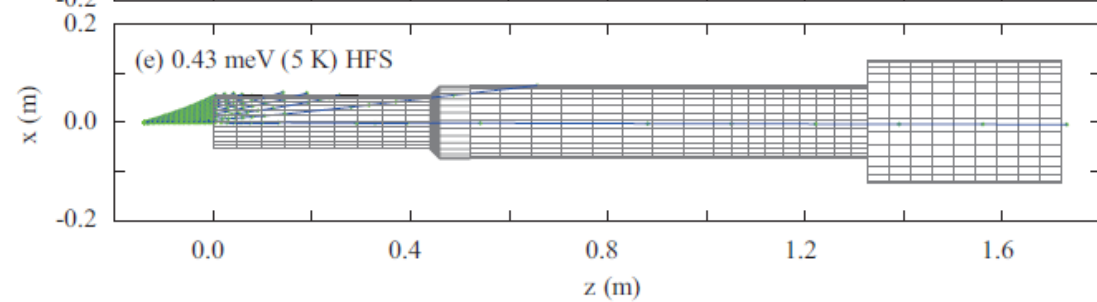
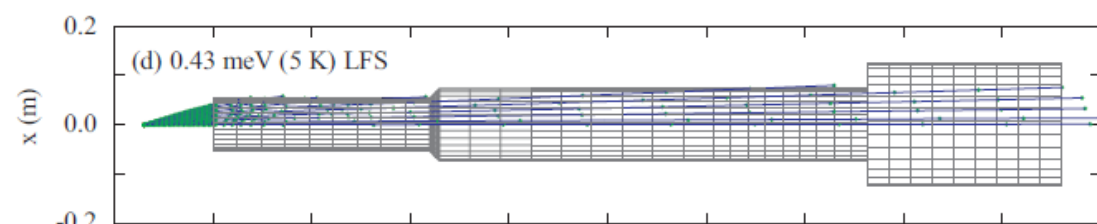
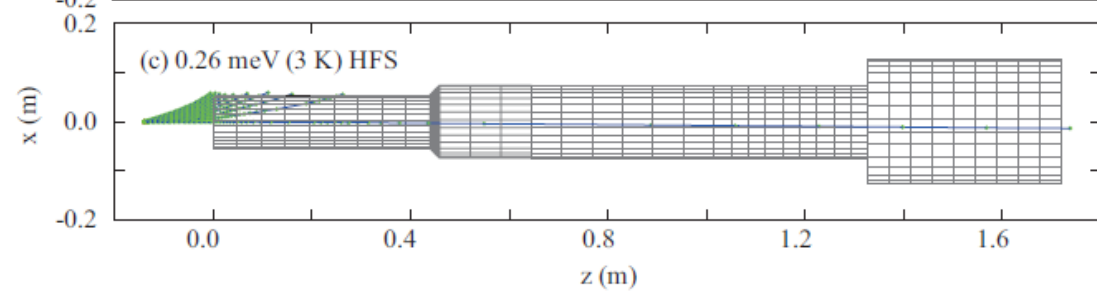
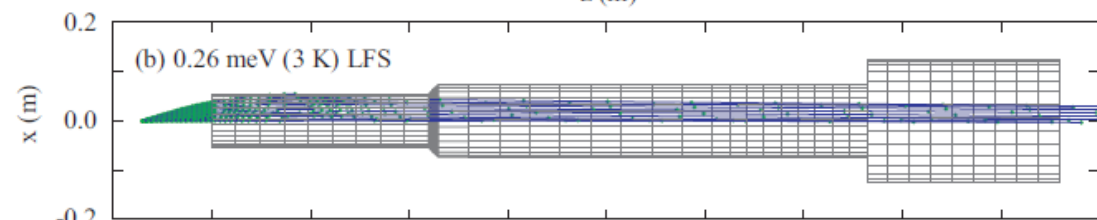
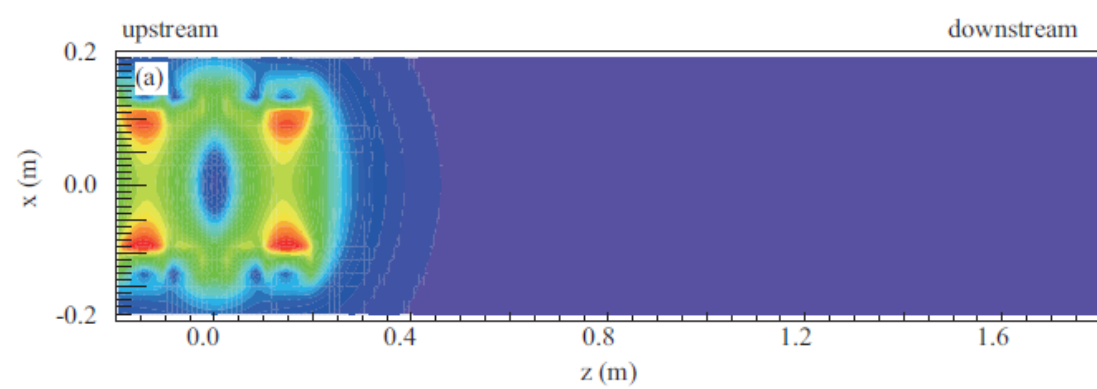
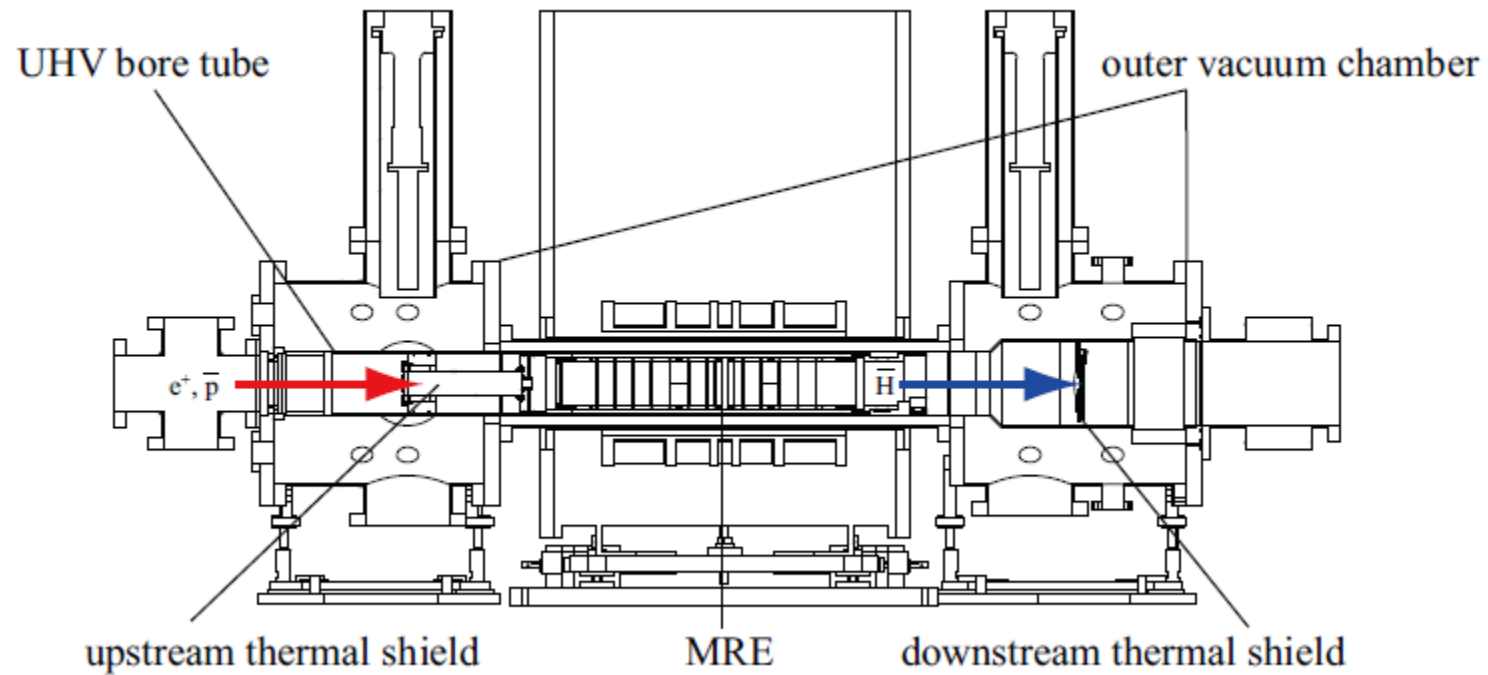


Figure 2.4: A schematic view of the coils to generate the cusp magnetic field with direction of the current and magnetic field lines.



Cross sectional drawing of cusp trap



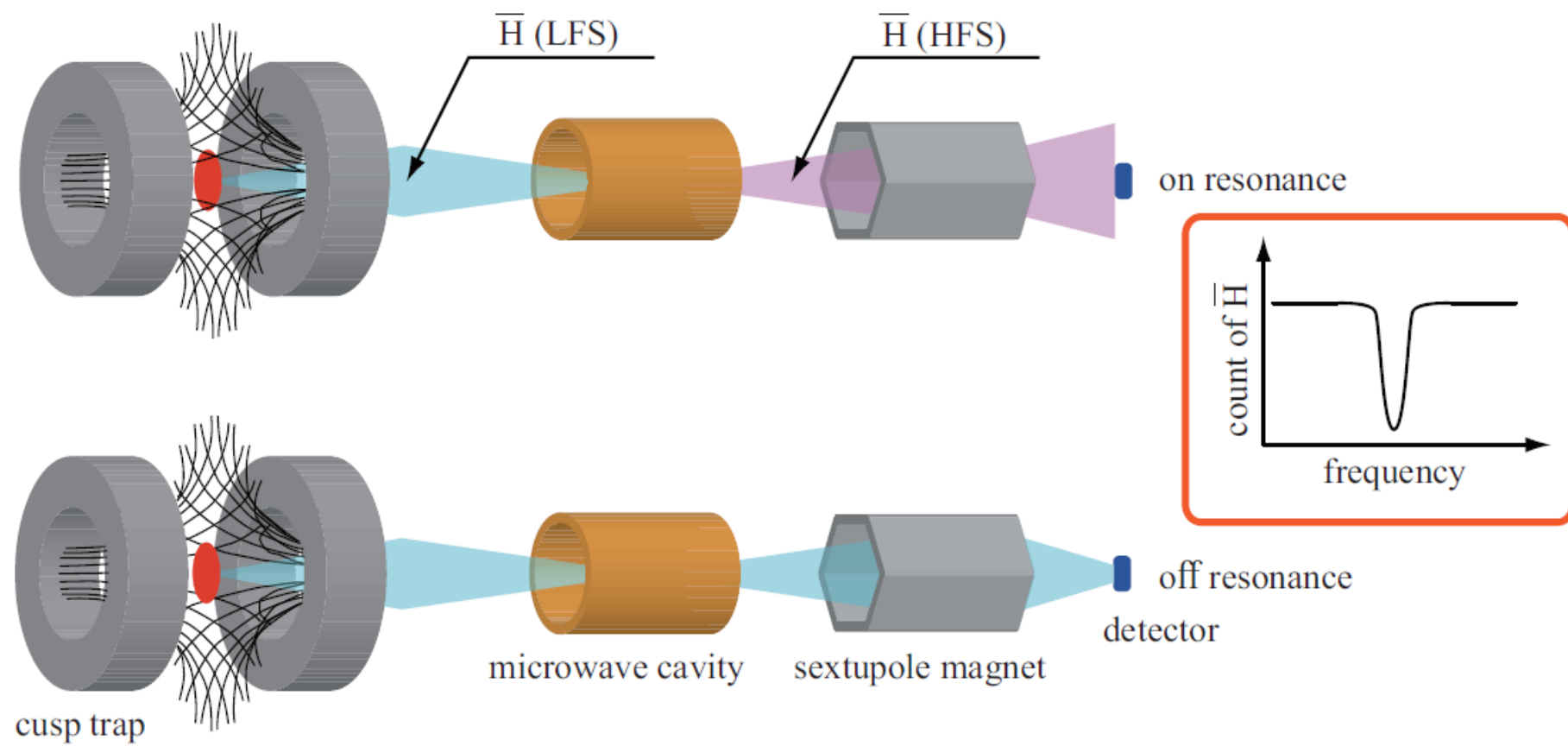
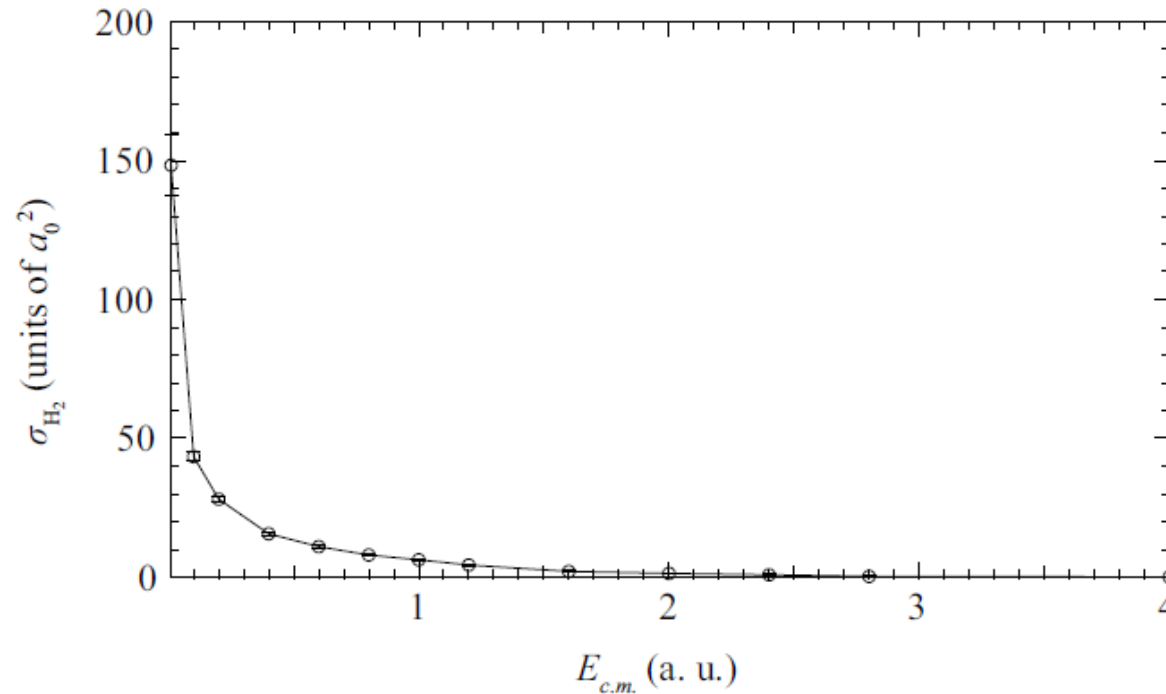


Figure 2.10: A conceptual drawing of our method to measure the ground state hyperfine splitting of antihydrogen atoms. When the frequency of the microwave in the cavity matches with the transition frequency of the hyperfine splitting of the atom, the atom transits to the HFS and is defocused by the sextupole magnet while it does not match with the transition frequency, the atom stays in the LFS and is focused on the detector. The transition frequency is determined from the dip position of the count of antihydrogen atoms as shown in the inset.

Why UHV is needed

Collision frequency : $\nu_{H_2} = \sigma_{H_2} v n (/s)$

Cross section of hydrogen molecule and antiproton :



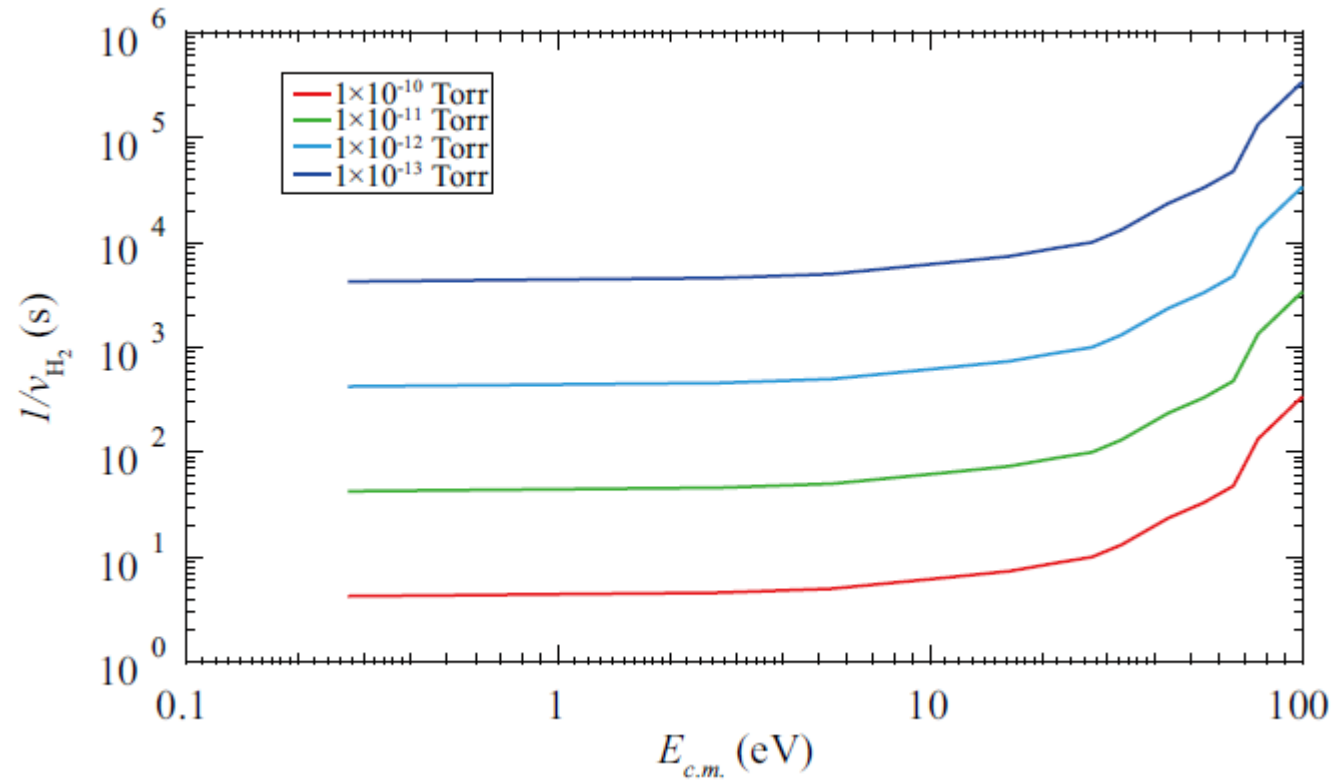
$$a_0^2 = 2.5 \times 10^{-21} (m^2)$$

$$\text{a. u.} = 931.494 (MeV/c^2)$$

J.S. Cohen. Molecular effects on antiproton capture by H_2 and the states of $p\bar{p}$ formed.
Physical Review A, 56(5):3583, 1997.

Number density of the hydrogen molecules : $n = N/V = P/kT$

Mean free time($1/v_{H_2}$) of antiproton for several different hydrogen pressures



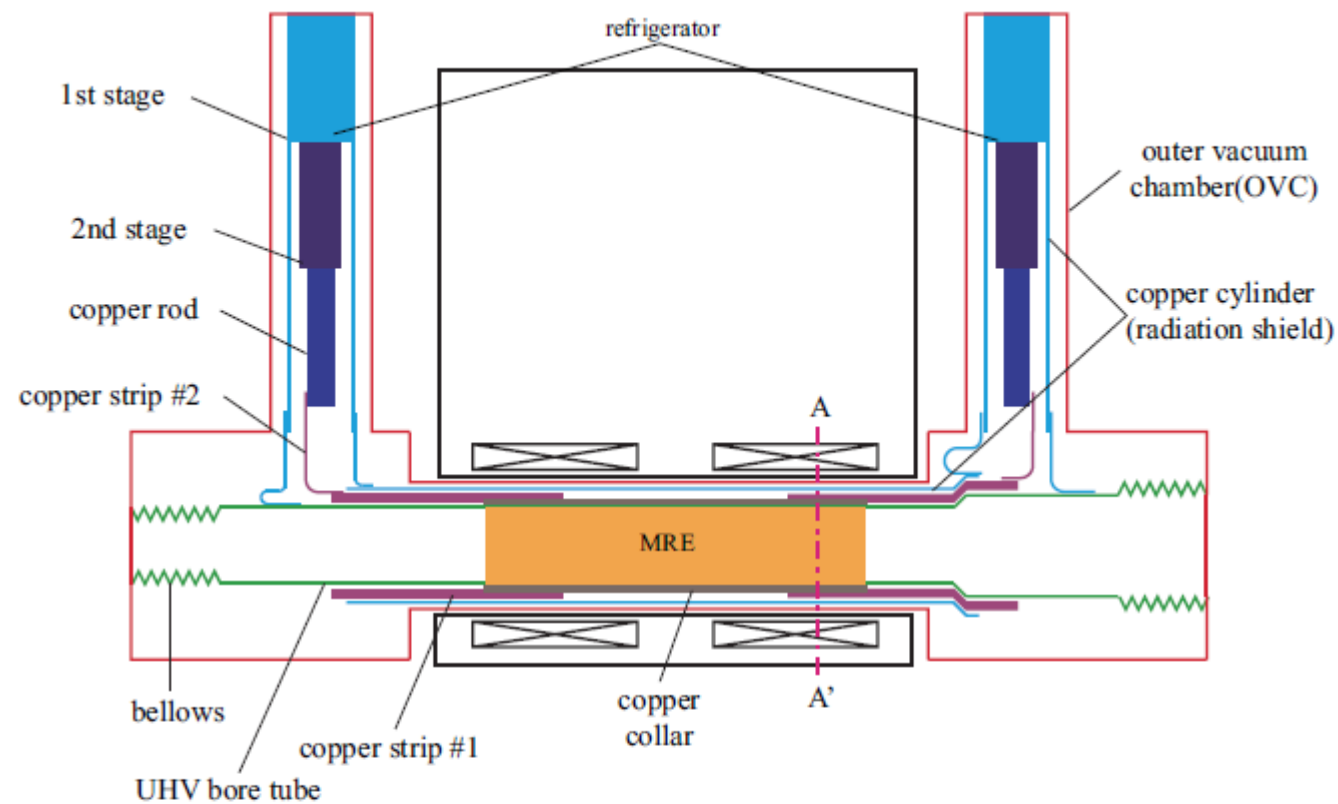


Figure 3.74: A schematic drawing of the UHV bore cooling system. The UHV bore tube is surrounded by the copper collar which is connected to the 2nd stages of the refrigerators by the copper rods and copper strips. The copper cylinders cover the copper collar, the strips, the rods and the 2nd stages of the refrigerators to shield thermal radiation. The cylinders are connected to the 1st stages of the refrigerators. The MRE is cooled via thermal contact with the UHV bore tube.

position	type	source	heat load
First stage	Radiation	Tube around refrigerator	400 mW
		tube around UHV bore	1100 mW
		upstream	1200 mW
		downstream	1100 mW
	conduction	upstream	1100 mW
		downstream	1000 mW
	total		6700 mW
Second stage	radiation	upstream	250 mW
		downstream	420 mW
	conduction	upstream	60 mW
		downstream	70 mW
	total		800 mW

Table 3.15: List of heat load to the UHV bore tube.

manufacturer	Iwatani
type	HE15
cooling power at 4.2 K	1.5 W
cooling power at 30 K	15 W
reachable temperature without heat load	3.2 K

